Synthesis, crystal structure, infrared and Raman spectra of $Sr_4Cu_3(AsO_4)_2(AsO_3OH)_4 \cdot 3H_2O$ and $Ba_2Cu_4(AsO_4)_2(AsO_3OH)_3$

Tamara Đorđević [a,*], Ljiljana Karanović [b]

[a] Institut für Mineralogie und Kristallographie, Universität Wien, Althanstrasse 14, A-1090 Wien, Austria
[b] Laboratory of Crystallography, Faculty of Mining and Geology, Đušina 7, 11000 Belgrade, Serbia

ABSTRACT

The two new compounds, $Sr_4Cu_3(AsO_4)_2(AsO_3OH)_4 \cdot 3H_2O$ (**1**) and $Ba_2Cu_4(AsO_4)_2(AsO_3OH)_3$ (**2**), were synthesized under hydrothermal conditions. They represent previously unknown structure types and are the first compounds synthesized in the systems $SrO/BaO–CuO–As_2O_5–H_2O$. Their crystal structures were determined by single-crystal X-ray diffraction [space group $C2/c$, $a = 18.536(4)$ Å, $b = 5.179(1)$ Å, $c = 24.898(5)$ Å, $\beta = 93.67(3)°$, $V = 2344.0(8)$ Å^3, $Z = 4$ for **1**; space group $P4_2/n$, $a = 7.775(1)$ Å, $c = 13.698(3)$ Å, $V = 828.1(2)$ Å^3, $Z = 2$ for **2**]. The crystal structure of **1** is related to a group of compounds formed by $Cu^{2+}–(XO_4)^{3-}$ layers ($X = P^{5+}$, As^{5+}) linked by M cations (M = alkali, alkaline earth, Pb^{2+}, or Ag^+) and partly by hydrogen bonds. In **1**, worth mentioning is the very short hydrogen bond length, $D \cdots A = 2.477(3)$ Å. It is one of the examples of extremely short hydrogen bonds, where the donor and acceptor are crystallographically different. Compound **2** represents a layered structure consisting of Cu_2O_8 centrosymmetric dimers crosslinked by $As1\phi_4$ tetrahedra, where ϕ is O or OH, which are interconnected by Ba, As2 and hydrogen bonds to form a three-dimensional network. The layers are formed by Cu_2O_8 centrosymmetric dimers of CuO_5 edge-sharing polyhedra, crosslinked by $As1O_4$ tetrahedra. Vibrational spectra (FTIR and Raman) of both compounds are described. The spectroscopic manifestation of the very short hydrogen bond in **1**, and ABC-like spectra in **2** were discussed.

© 2008 Elsevier Inc. All rights reserved.

1. Introduction

Natural and synthetic metal phosphates, arsenates and vanadates often form tetrahedral–octahedral framework structures with potentially interesting properties (e.g., ion conductivity, ion exchange and catalytic activities). An ongoing comprehensive study on hydrothermal synthesis, crystallography and properties of arsenate and vanadate (V) compounds in the insufficiently known system $M1O–M2O–X_2O_5–H_2O$ ($M1 = Sr^{2+}$, Cd^{2+}, Ba^{2+}, Bi^{3+}, Hg^{2+}; $M2 = Mg^{2+}$, $Mn^{2+,3+}$, $Fe^{2+,3+}$, Co^{2+}, Ni^{2+}, Cu^{2+}, Zn^{2+}; $X = As^{5+}$, V^{5+}) yielded a large number of new $M1^{2+}$–, $M2^{2+}$– and $M1–M2–(H−)$ arsenates and vanadates [1–10] that are characterized structurally, and, in part, also by spectroscopic techniques.

The previous investigations in the system $MO–CuO–X_2O_5–H_2O$, where M = alkaline-earth ion and X = P, V and As have revealed only a couple of compounds: tangeite, $CaCu(VO_4)(OH)$ [11,12], conichalcite, $CaCu(AsO_4)(OH)$ [13,14] nissonite, $Cu_2Mg_2(PO_4)_2(OH)_2(H_2O)_5$ [15], $BaCu_2(PO_4)_2(H_2O)$ and $Ba_2Cu(PO_4)_2(H_2O)$

[16] as well as vésigniéite, $BaCu_3(VO_4)_2(OH)_2$ [17]. The crystal structures of $CaCu(VO_4)(OH)$ and $CaCu(AsO_4)(OH)$ (both in space group $P2_12_12_1$, adelite structure type) consist of a three-dimensional assemblage of distorted VO_4/AsO_4 tetrahedra, $CuO_4(OH)_2$ tetragonal bipyramids and $CaO_7(OH)$ square antiprisms, sharing corners and edges. $Cu_2Mg_2(PO_4)_2(OH)_2(H_2O)_5$ (space group $C2/c$) consists of thick heteropolyhedral slabs parallel to (100), linked solely by a network of hydrogen bonds. Each slab consists of a sheet of corner-sharing ($Cu\phi_{10}$) dimers (ϕ = unspecified anions) sandwiched between two $[M(T\phi_4)\phi_3]$ sheets of corner-sharing ($Mg\phi_6$) and ($P\phi_4$) polyhedra. $BaCu_2(PO_4)_2(H_2O)$ and $Ba_2Cu(PO_4)_2(H_2O)$ (space groups $P2_12_12_1$ and $I2/a$, respectively) are related to a group of compounds formed by $Cu^{2+}–PO_4/AsO_4$ layers linked by cations with large ionic radii, and partly by hydrogen bonds. The layers are formed by Cu_3O_{12} units built from one CuO_4 square, which is corner-connected to two CuO_5 polyhedra, where Cu atoms are in a (4+1) or (3+2) coordination. $Ba_2Cu(PO_4)_2(H_2O)$ features isolated CuO_4 squares interconnected by PO_4 tetrahedra to chains which represent a component of the layers found in other compounds. The crystal structure of $BaCu_3(VO_4)_2(OH)_2$ (space group $C2/m$) is mainly composed of CuO_6 polyhedra linked to layers, with Ba ions located between them. Edge-sharing CuO_6 tetragonal bipyramids form chains parallel to (010) and (110); the

* Corresponding author. Fax: +43 1 4277 9532.
E-mail address: tamara.djordjevic@univie.ac.at (T. Đorđević).

chains are interlocked to form layers parallel to (001). Each of the VO_4 tetrahedra is linked by three CuO_6 and one BaO_{12} polyhedra. There are couple other compounds, such as $Ca_5(PO_4)_3$ $Cu_{0.27}O_{0.86}H_y$, $Ba_5(PO_4)_3Cu_{0.27}O_{0.86}H_y$, r'-$Ca_{19}Cu_2H_{1.42}(PO_4)_{14}$, and r''-$Ca_{19}Cu_{2-y}H_{2.24}(PO_4)_{14}$ $(0.64 \leqslant y \leqslant 0.7)$ [18,19], where only a part of copper has oxidation state 2+. Consequently, they do not belong to the $M1O$–CuO–X_2O_5–H_2O system.

The present contribution reports the hydrothermal synthesis and crystal structures of the two previously unknown compounds. Furthermore, these compounds represent new structure types. Raman and infrared spectra were acquired to obtain further information on both anion groups and especially on the very short hydrogen bond distances, where the donor and acceptor atoms are not equal due to (average) space-group symmetry. Besides potentially interesting properties, continuous investigations on the crystal chemistry of the arsenates are performed because arsenic is at the top of the priority of the most hazardous substances, but little is known about its crystal structures.

2. Experimental

2.1. Synthesis

In course of experiments to synthesize the divalent metal arsenates using hydrothermal method, the single crystals of two new compounds, $Sr_4Cu_3(AsO_4)_2(AsO_3OH)_4 \cdot 3H_2O$ (compound **1**) and $Ba_2Cu_4(AsO_4)_2(AsO_3OH)_3$ (compound **2**), were obtained from mixtures of $Sr(OH)_2 \cdot 8H_2O$ (Merck 7876, >97%), CuO (Merck 2768), As_2O_5 (Alfa Products 87687, >99.9%) and $Ba(OH)_2 \cdot 8H_2O$ (Mallinckrodt, 3772, >97%), $CuCO_3 \cdot Cu(OH)_2$ (distributor unknown), As_2O_5 (Alfa Products 87687, >99.9%). The mixtures were transferred into Teflon vessels and filled to approximately 75% of the inner volume with distilled water. Finally, they were enclosed into stainless-steel autoclaves. The mixture for **1** was heated under autogeneous pressure from 20 to 220 °C (3 h), held at that temperature (30 h) and finally cooled to room temperature (24 h). At the end of the reaction the pH of the solvent was 4, indicating moderate acidity. **1** crystallized as blue transparent prismatic crystals up to 0.15 mm in length (yield ca. 25%) accompanied with transparent, colorless, prismatic crystals of $Sr(AsO_3OH)$ (yield ca. 60%) [7] and uninvestigated amorphous mass (ca. 15%). The mixture for **2** was heated under autogeneous pressure from 20 to 220 °C (2 h), held at that temperature (24 h), then cooled to 100 °C (14 h), kept at that temperature (24 h), and finally cooled to room temperature (4 h). The reaction products were filtered, washed thoroughly with distilled water and dried in air at room temperature. At the end of the reaction the pH of the solvent was 3 indicating moderate acidity. **2** crystallized as transparent, turquoise, prismatic crystals up to 0.2 mm in length (yield ca. 35%). It was obtained together with acicular, blue crystals of $BaCu_2As_2O_7$ (yield ca. 60%) [20] and uninvestigated amorphous mass (ca. 5%).

2.2. X-ray diffraction experiments and crystal structure solution

The crystal quality of several single crystals of **1** and **2** were checked with a Nonius Kappa CCD single-crystal four-circle diffractometer (Mo tube, graphite monochromator, CCD detector frame size: 621 × 576 pixels, binned mode), equipped with a 300 μm diameter capillary-optics collimator. Each one sample exhibiting sharp reflection spots was chosen for data collection. A complete sphere of reciprocal space (φ and ω scans) was measured at room temperature (see Table 1 for details). For a **2** low-temperature measurement at 120 K was additionally

performed. This measurement resulted, as usual, in a little smaller unit cell. The hydrogen bonds found at the room temperature studies were maintained. Structural data of the refinements at low-temperature are deposited as supplementary material. The intensity data were processed with the Nonius program suite DENZO-SMN [21] and corrected for Lorentz, polarization, and background effects and, by the multi-scan method [21,22], for absorption.

The crystals of **1** showed a centered monoclinic unit cell. The space-group symmetry $C2/c$ was found from the extinction rules and confirmed by structure refinements. The crystal structure was solved by direct methods and refined using standard procedures [23,24]. Anisotropic displacement parameters were allowed to vary for all non-hydrogen atoms. However, the anisotropies were found to be only moderate. All five H atoms were found in a difference Fourier map and successfully refined, three of them with restraints on the O–H bond distances [OW1–H3/4 = 0.89(2) and O34–H2 = 0.89(2) Å]. Crystal data, information on the data collection and results of the final structure refinement are compiled in Table 1. The positional and displacement parameters are given in Table 2, bond distances and bond angles in Table 4.

The crystals of **2** all showed cell parameters according to a primitive tetragonal metric, space-group symmetry $P4_2/n$ (origin at $\bar{1}$ on n, at $\frac{1}{4}, \frac{1}{4}, \frac{1}{4}$ from $\bar{4}$). The crystal structure was solved by direct methods and refined using standard procedures. Anisotropic displacement parameters were allowed to vary for all atoms; only for the H atom, which was located in a difference Fourier map, the isotropic displacement parameter was refined with restraint on the O–H [O5–H = 0.89(2)]. Crystal data, information on the data collection and results of the final structure refinement are compiled in Table 1. The positional and displacement parameters are given in Table 3, bond distances and bond angles in Table 5. All molecular drawings were produced with ATOMS [42].

2.3. Infrared and Raman spectra

In order to investigate the hydrous species polarized single-crystal infrared spectra were recorded on a Bruker Tensor 27 FTIR spectrophotometer with mid-IR glowbar light source and KBr beam splitter, attached to a Hyperion 2000 FTIR microscope with liquid nitrogen-cooled mid-IR, broad band MCT detector. A total of 128 scans were accumulated between 4000 and 530 cm^{-1} circular sample aperture 100 μm diameter and ATR 15 × objective.

In order to study the arsenate groups Raman spectra were measured with a Renishaw RM1000 notch filter-based micro-Raman system in the spectral range from 4000 to 200 cm^{-1}. The 514.5 nm excitation line of a 20 mW Ar ion laser was focused with a 50 × /0.75 objective on the crystal faces of the single crystals. Raman intensities were collected with a thermo-electrically cooled CCD array detector. The sample spectra were acquired with a nominal exposure time of 30 s (resolution: 4–5 cm^{-1}; mode: continuous grating scan mode, 1200 lines/mm grating).

3. Results and discussion

3.1. $Sr_4Cu_3(AsO_4)_2(AsO_3OH)_4 \cdot 3H_2O$

The crystal structure of **1** can be divided into two types of structural slabs parallel to the (001) plane (Fig. 1). Slab A is placed between the z coordinates from about −0.15 to about 0.15. This slab is composed of Cu_3O_{12} groups interconnected by $As2O_4$ and $As3O_3OH2$ coordination tetrahedra, similar to those found in related phosphates [16 and references therein], where different

Table 1
Crystal data, data collection and refinement details for **1** and **2**

Crystal data			
Chemical formula	$Sr_4Cu_3(AsO_4)_2(AsO_3OH)_4 \cdot 3H_2O$	$Ba_2Cu_4(AsO_4)_2(AsO_3OH)_3$	
Temperature	293 K	293 K	120 K
Formula weight, M_r (g/mol)	1432.70	1226.46	1226.46
Space group (no.), Z	$C2/c$ (15), 4	$P4_2/n$ (86), 2	$P4_2/n$ (86), 2
a (Å)	18.536(4)	7.790(1)	7.775(1)
b (Å)	5.1790(10)	7.790(1)	7.775(1)
c (Å)	24.898(5)	13.702(3)	13.698(3)
β (°)	101.28(3)	–	–
V (Å^3)	2344.0(8)	831.5(2)	828.1(2)
Calculated density D_x (g/cm^3)	4.060	4.899	4.919
Absorption coefficient, μ (mm^{-1})	20.229	19.669	19.750
T_{min}/T_{max}	0.2369/0.2945	0.1564/0.2705	0.1556/2695
Crystal size (mm^3)	$0.10 \times 0.10 \times 0.08$	$0.15 \times 0.15 \times 0.09$	$0.15 \times 0.15 \times 0.09$
Data collection			
Crystal-detector distance (mm)	30	31	31
Rotation width (°)	2	1.5	1.5
Total no. of frames	427	660	450
Collection time per frame (s)	180	140	180
Absorption correction	Multi-scan		Multi-scan
Reflections collected/unique	6494/3420	3554/1842	13614/1824
Observed reflections [$I> 2\sigma(I)$]	2864	1710	1712
R_{int}	0.0172	0.0152	0.0374
θ_{max} (°)	30.034	34.95	34.95
Refinement			
Extinction coefficient, k^a	0.00046(2)	0.0025(2)	0.0016(2)
Refined parameters	201	76	76
R-indices [$I>2\sigma(I)$]	$R_1 = 0.0206$	$R_1 = 0.0213$	$R_1 = 0.0280$
	$wR_2 = 0.0510$	$wR_2 = 0.0528$	$wR_2 = 0.0720$
R-indices (all data)	$R_1 = 0.0288$	$R_1 = 0.0241$	$R_1 = 0.0308$
	$R_2 = 0.0542$	$wR_2 = 0.0537$	$wR_2 = 0.0731$
Goodness-of-fit, S	1.042	1.168	1.160
$(\Delta/\sigma)_{max}$	0.001	0.000	0.001
$(\Delta\rho)_{max}$, $(\Delta\rho)_{min}$ (e/Å^3)	0.902, −0.728	1.889; −1.309	3.78, −2.27
a, b^b	0.0273, 3.06442	0.0170, 2.3064	0.0292, 7.4535

[a] $F_c^* = kF_c[1+0.001 \times F_c^2\lambda^3/\sin(2\theta)]^{-1/4}$.
[b] $w = 1/[\sigma^2(F_0^2)+(aP)^2+bP]$.

Table 2
Fractional atomic coordinates and displacement parameters for **1**

Atom	X	y	Z	U_{equiv}
Sr1	0.129022(14)	0.51834(4)	0.406656(10)	0.00951(6)
Sr2	0.297704(14)	0.52007(5)	0.330227(11)	0.01310(7)
Cu1	0.150538(15)	0.02029(5)	0.295113(11)	0.01035(7)
Cu2	0.267498(14)	0.01626(5)	0.444328(10)	0.00739(7)
As1	−0.006302(14)	0.98112(5)	0.425444(11)	0.00797(7)
As2	0.0	0.5	0.5	0.01015(10)
As3	0.152892(19)	0.00172(5)	0.525778(14)	0.01042(8)
O11	0.21459(10)	0.1889(4)	0.27324(8)	0.0159(4)
O12	0.17570(10)	0.7555(4)	0.33142(8)	0.0160(4)
O13	0.08983(10)	0.1982(3)	0.32314(8)	0.0144(4)
O14	0.09950(12)	−0.0784(5)	0.23149(9)	0.0220(5)
O21	0.24202(9)	0.2501(3)	0.39801(7)	0.0117(4)
O22	0.31267(10)	0.7726(3)	0.42118(7)	0.0129(4)
O23	0.19198(9)	0.8859(4)	0.46276(7)	0.0123(4)
O24	0.17146(9)	0.3544(3)	0.50278(7)	0.0114(4)
O31	0.40578(9)	0.3912(4)	0.41829(8)	0.0125(4)
O32	0.01397(10)	0.2982(3)	0.43428(8)	0.0126(4)
O33	0.04545(9)	0.8014(3)	0.47566(8)	0.0115(4)
O34	0.02343(10)	0.8760(4)	0.36873(8)	0.0134(4)
OW1	0.37956(17)	0.9378(6)	0.33502(11)	0.0432(7)
OW2	0.0	0.5276(7)	0.25	0.0324(9)
H1	0.070(2)	−0.158(8)	0.2333(16)	0.035(12)
H2	0.0423(18)	1.013(5)	0.3535(14)	0.020
H3	0.396(2)	0.994(7)	0.3677(10)	0.049
H4	0.409(2)	1.001(7)	0.3172(17)	0.049
H5	0.027(2)	0.446(8)	0.2714(19)	0.053(14)

U_{equiv} according to [39].

Table 3
Fractional atomic coordinates and displacement parameters for **2** for the room temperature data collection

Atom	x	y	z	U_{equiv}
Ba	0.75	0.25	0.174635(17)	0.01284(7)
Cu	0.17540(4)	0.06542(4)	0.05429(2)	0.00865(7)
As1	0.67802(3)	0.50863(3)	0.404045(19)	0.00757(7)
As2	0.25	0.25	0.25	0.00686(9)
O1	0.5547(3)	0.6799(3)	0.42963(15)	0.0130(4)
O2	0.5681(3)	0.3339(3)	0.37279(14)	0.0132(4)
O3	0.8241(2)	0.4752(3)	0.49293(14)	0.0111(3)
O4	0.4050(2)	0.3293(3)	0.17623(13)	0.0113(3)
O5	0.7869(3)	0.5406(3)	0.29626(17)	0.0183(4)
H	0.841(9)	0.640(5)	0.296	0.05(2)

U_{equiv} according to [39].
Note: The occupancy factor of the H atom is 0.75.

patterns and links of the Cu_3O_{12} groups by PO_4 tetrahedra were observed. Like in $Sr_3Cu_3(PO_4)_4$ [16], Cu_3O_{12} groups are oriented parallel to each other due to translation symmetry (Fig. 2) and form an *AB* stacking sequence. Sr1O$_7$OH2 polyhedra are sitting in the holes of the network formed by coordination polyhedra of Cu and As atoms.

Slab *B* is built of Sr2O$_6$OH1OW1 polyhedra and As1O$_3$OH1 coordination tetrahedra plus an uncoordinated water molecule OW2. Both hydroxyl groups (OH1, OH2) and water molecules
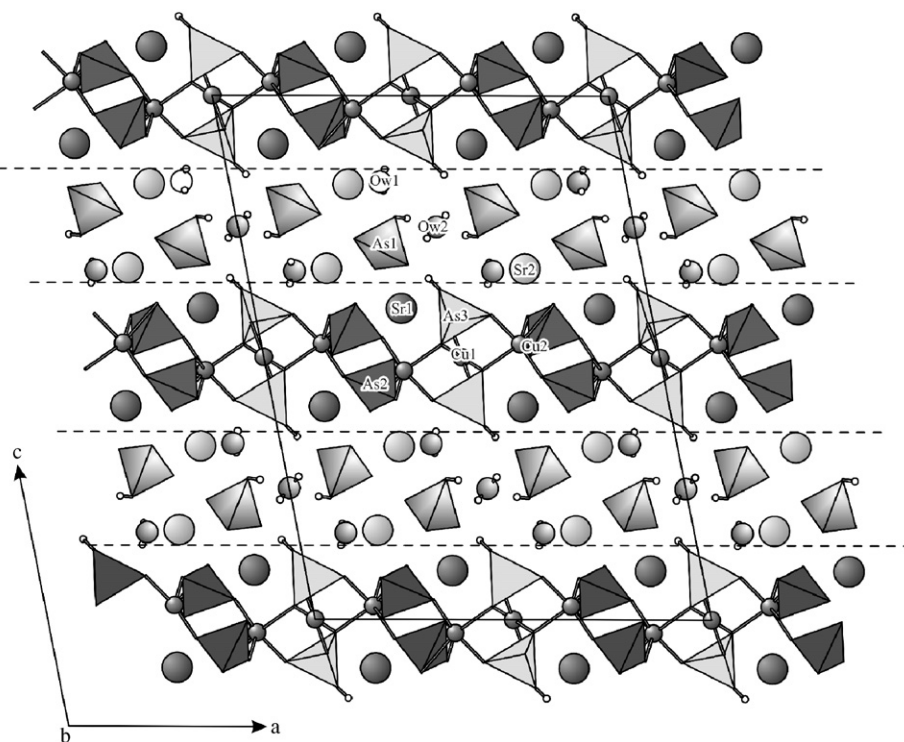
Fig. 1. Crystal structure of **1** projected along [010] showing *ABAB* arrangement of the two parallel slabs.

(OW1, OW2) in **1** form hydrogen bonds, which are mainly located in the *B* slab. Its boundaries lie between *z* about 0.15 and 0.35. These slabs show an *ABAB* stacking sequence along *c* (Fig. 1).

A central part of a Cu_3O_{12} group is the Cu1 atom, which is coordinated by four O atoms (two symmetry-equivalents of O32 and O33), adopting a square planar coordination with the average $\langle Cu1-O \rangle$ bond length of 1.964 Å (Fig. 2). The O–Cu1–O angles of neighboring O atoms deviate up to 2° from the ideal value of 90°. For the opposite O atoms, O–Cu1–O angles are symmetrically constrained to exactly 180° (site symmetry $\bar{1}$). The $Cu1O_4$ coordination polyhedron shares two opposite O atoms with two symmetry-equivalent $Cu2O_5$ coordination polyhedra and another two O atoms with $As3O_3OH2$ tetrahedra. The Cu1–Cu2 distance is 3.8058(9) Å. The Cu2 atom is coordinated by five O atoms adopting a [4+1] coordination which can be described as a square pyramid. In the tetrahedrally distorted basal plane Cu2 has the four nearest O atoms at distances of 1.947(2)–2.006(2) Å. The fifth apical O atom is at a longer distance of 2.372(2) Å. In the basal plane the O–Cu–O angles between neighboring O atoms range from 83.22(8)° to 101.31(8)°, and between the opposite O atoms they are 144.87(8)° and 169.28(8)°. Considering these angles the coordination polyhedron can also be considered as an example of the transition from a tetragonal pyramidal (4+1) towards a trigonal bipyramidal (3+2) coordination (Fig. 2). A similar configuration was found in [25].

The coordination polyhedra of the Sr atoms are irregular. Both the $Sr1O_7OH2$ and $Sr2O_6OH1OW1$ polyhedra represent square antiprisms with average $\langle Sr1/2-O \rangle$ bond lengths of 2.630 Å each. The individual values range from 2.510(2) to 2.923(2) Å. The top and bottom faces of the Sr1/2 polyhedra are formed by the atoms O32–O13–O21–O24 and O33–O34H2–O12–O23/O14H1–O31–O21–O11 and $O11^i$–OW1–O22–O12, respectively. The gap to further ligands is significant; further distances to O atoms are $\geqslant 3.60/3.37$ Å, respectively. The sum of bond valences for the Sr1 atom suggest a slight oversaturation if all eight ligands are considered (Table 6). However, neglecting the

longest of the Sr1–O distances gives an unsatisfactory bond-valence sum for the O33 atom.

Sharing a common edge (O12–O21) one $Sr1O_7OH2$ and one $Sr2O_6OH1OW1$ coordination polyhedra build up a pair of $Sr1\phi_8Sr2\phi_8$ polyhedra, where ϕ is O, OH or H_2O. The Sr1–Sr2 distance in a pair is 3.9656(9) Å. Each such pair is bonded to another pair of $Sr1\phi_8Sr2\phi_8$ polyhedra sharing common vertices (O11 and its symmetry-equivalents) and forming ziz-zag chains in the direction of the monoclinic twofold crystallographic *b*-axis (Fig. 3). In that way, every $Sr2\phi_8$ polyhedron shares a common edge with one $Sr1\phi_8$ polyhedron and two common vertices with two neighboring $Sr2\phi_8$ polyhedra. Inside the chains, $Sr1\phi_8Sr2\phi$ polyhedra are additionally connected by hydrogen bonds involving the hydroxyl group OH2 and coordinated water molecule OW1: O34–H2···O13, OW1–H3···O31 and OW1–H4···O14 (Fig. 4). With a distance of 2.477(3) Å the hydrogen bond O34–H2···O13 is considered as very strong H bond [26]. The two hydrogen bonds of the coordinated water molecule OW1 are weak [OW1–H3···O31 = 3.107(3) and OW1–H4···O14 = 3.069(4) Å]. The OW1–H···O angles are bent due to the strong connection of OW1 to Sr2. Two neighboring zig-zag chains are interconnected by hydrogen bonds linking the uncoordinated water molecule OW2. OW2 lies on the inversion center and acts as a double hydrogen bond donor toward the two symmetry-equivalent oxygen atom O13 from the $As1O_3OH1$ group and as a double hydrogen bond acceptor of two symmetry-equivalent OH1 groups connecting two $As1O_3OH1$ tetrahedra (Fig. 4). The hydrogen bonds OW2–H5···O13 and O14–H1···OW2 are more or less linear.

In the space between two adjacent zig-zag chains, besides OW2, coordination polyhedra of As and Cu atoms are situated. The coordination figures around three As atoms represent three distinct tetrahedra. All of them have site symmetry 1. The average $\langle As-O/OH \rangle$ bond lengths are very similar: 1.692, 1.687 and 1.690 Å. However, the individual As–O bond lengths vary from 1.650(2) to 1.706(2) Å, but the As–OH bond (As1–O14) is distinctly longer: 1.755(2) Å. Consequently, two protonated arsenate groups,
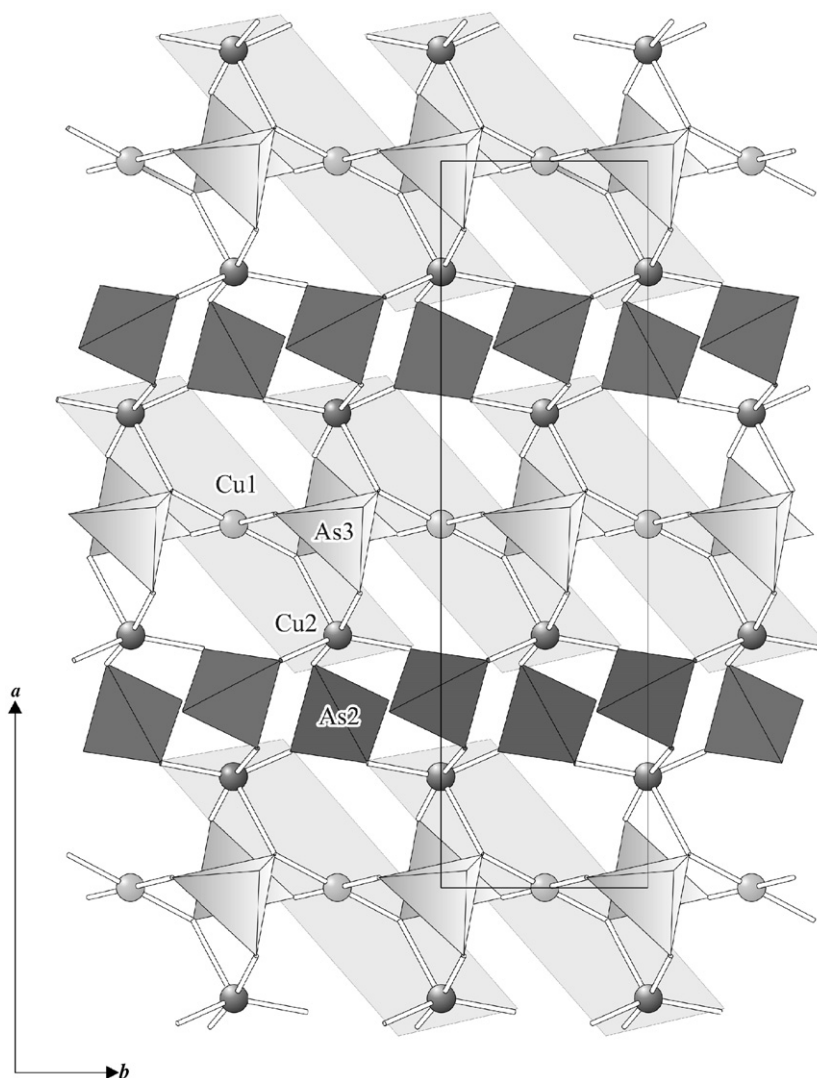
Fig. 2. The connection of Cu(II) atoms and arsenate tetrahedra in **1**: the Cu_3O_{12} groups are arranged parallel to each other.
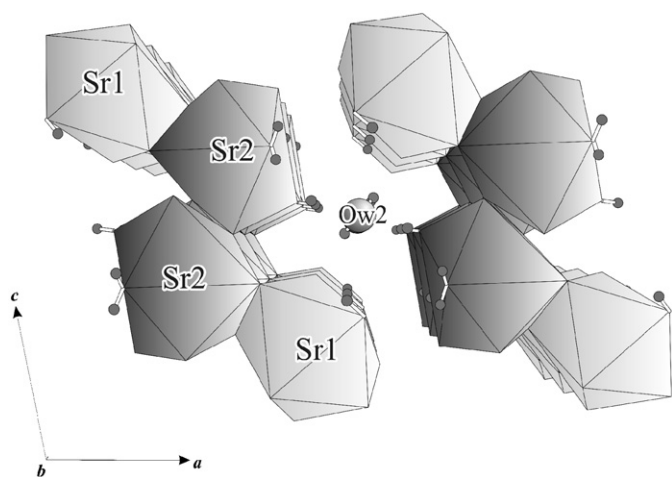

Fig. 3. The zig-zag chains of $Sr1\phi_8Sr2\phi_8$ polyhedra in **1**, (ϕ = O, OH or H_2O) in the direction of the *b*-axis.
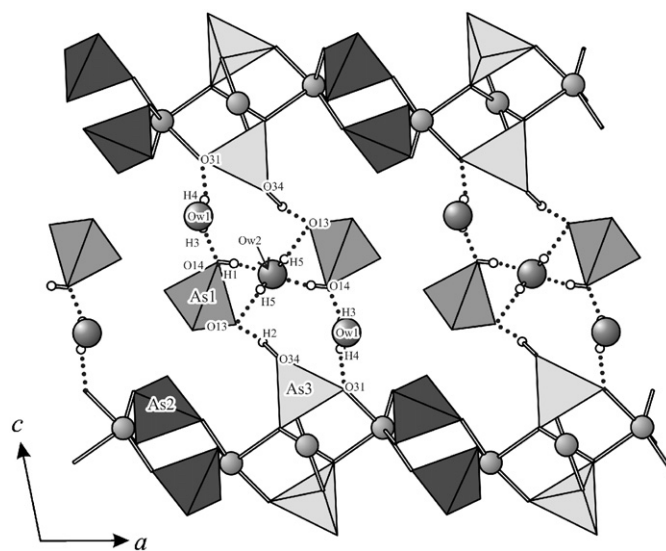

Fig. 4. The hydrogen bonds in **1**.

As1O$_3$OH1 and As3O$_3$OH2, besides a pure arsenate tetrahedron As2O$_4$, were identified. Ferraris and Ivaldi [27] found for 36 well-determined monoprotonated arsenate groups an average ⟨As–OH⟩ distance of 1.731(2) which is somewhat shorter than 1.755(2) Å found in **1**. The explanation is given by the fact that besides As1 and H1, the O14 atom is additionally bonded to Sr2 and it is also a single hydrogen bond acceptor from the coordinated water molecule OW1, which provides a comparably large contribution to the bond valence. The bond-valence sum for O14 formally is slightly oversaturated (2.18 v.u.), and as a consequence, a relatively long As1–O14 bond is caused in **1**. The O–As1–O angles are consistent with this interpretation. As compared with the ideal tetrahedral angle of 109.47°, O–As1–O14 angles are slightly smaller [ranging from 98.75(11)° to 107.20(11)°] or slightly larger [ranging from 111.18(9)° to 118.28(10)°]. A similar crystal-chemical behavior was found for protonated phosphate groups [28].

The As2O$_4$ tetrahedron is much more regular than the protonated ones, with O–As2–O angles ranging between 105.17(9)° and 114.04(9)°.

The second protonated tetrahedron As3O$_3$OH2 shows an As3–O34 distance of 1.703(2), which is somewhat shorter than the already mentioned average ⟨As–OH⟩ distance of 1.731(2) Å [27]. Nevertheless, the hydrogen atom H2 is covalently bonded to O34. With a distance of 2.477(3) Å the hydrogen bond O34–H2···O13 is considered as very strong H bond. Taking into account the contribution of non-hydrogen atoms only, the O34 and O13 atoms are both undersaturated, i.e., v_{ij}(O34) and v_{ij}(O13) are 1.38 and 1.42 v.u., respectively. Taking into account that the O34 atom is the single donor of a very strong hydrogen bond toward O13, and that the O13 atom is the double hydrogen bond acceptor of one strong and one weak hydrogen bond from O34 and OW2, respectively, the bond valences are well balanced. The angle O34–H2···O13 of 165(3)° is in accordance with an only slightly bent hydrogen bond. The hydrogen bonding geometry is given in Table 4 and Fig. 4 and it is in accordance with the bond valences (Table 6).

Table 4
Selected bond distances (Å) and bond angles (°) for the coordination polyhedra in **1**

Sr1–O24	2.510(2)	Cu1–O33	1.927(2)	As1–O11	1.650(2)
–O23	2.516(2)	–O33^{iii}	1.927(2)	–O12^{ii}	1.658(2)
–O12	2.530(2)	–O32^{iii}	2.001(2)	–O13	1.706(2)
–O21	2.557(2)	–O32	2.001(2)	–O14	1.755(2)
–O32	2.626(2)	⟨Cu1–O⟩	1.964	⟨As1–O⟩	1.692
–O13	2.648(2)				
–O34	2.726(2)	Cu2–O23^{ii}	1.947(2)	As2–O21	1.676(2)
–O33	2.923(2)	–O22^{iv}	1.960(2)	–O22^{ii}	1.678(2)
⟨Sr1–O⟩	2.630	–O24	1.965(2)	–O23^{ii}	1.696(2)
		–O31^{iv}	2.006(2)	–O24^{iv}	1.697(2)
Sr2–O11	2.544(2)	–O33^{ii}	2.372(2)	⟨As2–O⟩	1.687
–O21	2.559(2)	⟨Cu2–O⟩	2.05		
–O12	2.575(2)			As3–O31^{v}	1.671(2)
–O22	2.582(2)			O32^{vi}	1.689(2)
–OW1	2.632(2)			O33	1.697(2)
–O11^{i}	2.688(2)			O34	1.703(2)
–O14^{i}	2.720(2)			⟨As3–O⟩	1.690
–O31	2.747(2)				
⟨Sr2–O⟩	2.630				

Hydrogen bonds

Donor (D)	H atom	Acceptor (A)	D–H	H···A	D–H···A	D···A
O14	H1	OW2^{vi}	0.70(4)	2.17(4)	163(4)	2.847(4)
O34	H2	O13	0.90(2)	1.60(2)	163(3)	2.477(3)
OW1	H3	O31^{vii}	0.86(2)	2.40(3)	139(3)	3.106(3)
	H4	O14^{viii}	0.83(2)	2.35(3)	146(4)	3.072(4)
OW2	H5	O13	0.75(4)	2.04(4)	175(4)	2.797(3)

^{i} −x+1/2, y+1/2, −z+1/2; ^{ii} x, y−1, z; ^{iii} −x, −y+1, −z+1; ^{iv} −x+1/2, −y+1/2, −z+1; ^{v} x−1/2, y+1/2, z; ^{vi} x, y−1, z; ^{vii} x, y+1, z; ^{viii} x+1/2, y+1/2, z.
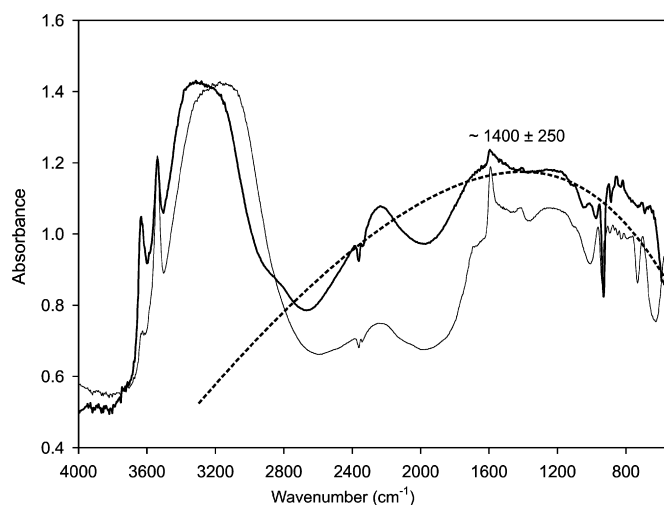

Fig. 5. Single-crystal infrared spectra of **1** on a (010) face (bold: parallel to the elongation, thin: perpendicular to the elongation). Bands < 1000 cm^{-1} truncated due to strong absorption.
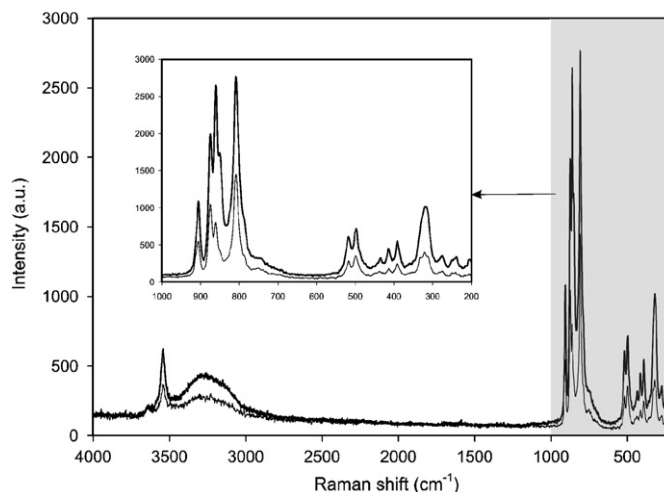

Fig. 6. Raman spectra of a (010) face of **1**.

To obtain further information on the anion groups and especially on hydrogen bonds polarized single-crystal infrared (4000–530 cm^{-1}) and Raman spectra (4000–70 cm^{-1}) on the (010) face were acquired (Figs. 5 and 6). Both the IR and the Raman spectra reflect the complexity of the crystal structure. The considerably large numbers of bands below 1000 cm^{-1}, which cannot be unambiguously assigned, are caused by the vibrations of three crystallographically different AsO$_4$ tetrahedra, of which two are protonated. Spectral data on orthoarsenates that have been previously published are so far rather incomplete [29] and not in good agreement with each other. Therefore, attempts to compare with them failed. However, the distinct frequency ranges may be assigned as follows: The spectral region between 3800 and 1000 cm^{-1} shows a peculiar increase in "background absorption" (Fig. 5), which is a typical feature of compounds with very short, i.e., very strong hydrogen bonds (e.g., mozartite [30], pectolite and serandite [31], natrochalcite-type compounds [32], and organic compounds [33]). It represents, an extremely broad (FWHM ∼1000 cm^{-1}) and low-energetic band that is assigned to the OH stretching mode of the very strong H bond O34–H2···O13. The peculiar shape of the band (large FWHM, wavy appearance, and transmission window at ∼2360 cm^{-1}) is caused by resonance

and interference phenomena enhanced by the strong anharmonicity [34] of this vibration. Because of the broad band shape, As–O tetrahedral stretching vibrations and lattice modes are superimposed in the low-energy region of the spectrum. The large FWHM aggravates a precise determination of the band center, which is estimated to be roughly at $\sim 1400 \pm 250\,cm^{-1}$. According to the d–v correlation for hydrogen bonds this wavenumber is in excellent agreement with the refined O34–H2···O13 bond length of only 2.477(3) Å [33,35]. All other O–H stretching frequencies in this region are in excellent agreement with d–v correlations for hydrogen bonds given in [35]. Very strong broad and partly truncated bands (FWHM$\sim$560 cm^{-1}) in infrared spectra at 3293 and 3161 cm^{-1} at two polarization directions, respectively, and one middle strong broad (FWHM$\sim$340 cm^{-1}). Raman band at 3259 cm^{-1} are in excellent agreement with moderately strong hydrogen bonds of 2.797(3) and 2.847(4) Å. Strong bands at 3540 cm^{-1} both in infrared and Raman spectra agree with a weak hydrogen bond of 3.072(4) Å and medium strong band at 3637 cm^{-1} in infrared and 3639 cm^{-1} in Raman agree with a weak hydrogen bond of 3.106(3) Å. The sharp bands at $\sim$1600 cm^{-1} in the IR spectra are assigned to the bending mode of the water molecule. Bands around 2360 cm^{-1} are assigned to the CO_2 impurities.

Due to strong absorption, bands below $\sim$1000 cm^{-1} are truncated in infrared spectra and therefore are not further discussed (there was not enough material for a powder IR measurement). In the 1000–700 cm^{-1} range, Raman spectra show the As–O stretching modes of the $(AsO_3OH)^{2-}$ and $(AsO_4)^{3-}$ groups. The intense bands around 905, 875 and 860 cm^{-1} correspond to the symmetric stretching vibrations of $(AsO_4)^{3-}$ and $(AsO_3OH)^{2-}$ groups. The very intense band at 808 cm^{-1} represents the antisymmetric stretching mode of the protonated arsenate group [9]. It has been suggested that the $(AsO_4)^{3-}$ group is the only tetrahedral oxyanion of the main group elements in which $v_{sym} > v_{asym}$ [29].

In the region below 550 cm^{-1} appear the bending modes of the $(AsO_3OH)^{2-}$ and $(AsO_4)^{3-}$ groups, and various low-energetic lattice modes of the compound.

3.2. $Ba_2Cu_4(AsO_4)_2(AsO_3OH)_3$

The asymmetric unit of **2** contains two cations (Ba at a special, and Cu at a general position) and two anions, i.e. two crystallographically non-equivalent arsenate groups, one of which is partly protonated. It represents a structure with copper arsenate layers normal to [001] interconnected by Ba, As2, and hydrogen bonds (Fig. 7).

The central part of layers in **2** is Cu_2O_8 centrosymmetric dimer, which contains two CuO_5 edge-sharing square pyramids. In one layer Cu_2O_8 dimers are arranged parallel to each other (Fig. 7), but in neighboring layers they are differently oriented, corresponding to operation of the 4_2 screw axis and n glide plane, so that succeeding layers form an *ABAB* stacking sequence. Cu_2O_8 centrosymmetric dimers are crosslinked by As1ϕ_4 tetrahedra, where ϕ is O or OH, forming channels along [001], which are in turn occupied by Ba and As2.

The core of the Cu_2O_8 centrosymmetric dimers are planar $[Cu_2O_2]$ clusters, which contain two Cu atoms bridged by two O3 atoms. These cores are terminated by six O atoms (three centrosymmetric pairs of O1, O2, O4). In the Cu_2O3_2 plane the Cu–Cu distance is 3.2740(8) Å, which is longer than 3.1020(8) Å between copper(II) cations in neighboring dimers, suggesting the larger cation–cation repulsion in the Cu_2O3_2 plane. The Cu–O3–Cu^i ($i = -x, -y, -z$) angle is 99.57(8)°. Similar layers formed by the Cu_2O_8 dimers crosslinked by PO_4 tetrahedra have been described for $NH_4CuPO_4 \cdot H_2O$ [36].

Similar to Cu2 in **1** the Cu atom in **2** is in a distorted square-pyramidal coordination, with the basal O atoms at distances in the range of 1.899(2)–2.048(2) Å. They form the tetrahedrally deformed basal plane with an average $\langle Cu-O \rangle$ bond length of 1.970 Å. As expected, the Cu atom is displaced towards the apical O3 atom at a longer distance of 2.309(2) Å. In the basal plane, the O–Cu–O angles between neighboring oxygen atoms range from 85.89(8)° to 95.61(8)°. One of the opposite O–Cu–O angles is only 154.44(8)°, whereas the other one is 168.20(9)°. Therefore, as in **1**, this coordination may be considered as an example for the transition from a tetragonal pyramidal (4+1) toward a trigonal bipyramidal (3+2) coordination [25].

The large cation Ba is bonded to 10 O atoms (five symmetry-equivalent pairs), six at shorter and four at longer distances with an average $\langle Ba-O \rangle$ bond length of 2.928 Å. The individual bond lengths range from 2.758(2) to 3.131(2) Å. The coordination polyhedron can be described as a bicapped distorted cube. It shares common edges with the two surrounding As1ϕ_4 and only vertices with another four As1ϕ_4 and two As2O_4 tatrahedra. Because of the site symmetry the Ba atom is situated perfectly in the center of the coordination polyhedron.

The two crystallographically distinct As atoms are tetrahedrally coordinated and have mean $\langle As-O \rangle$ bond distances of 1.688
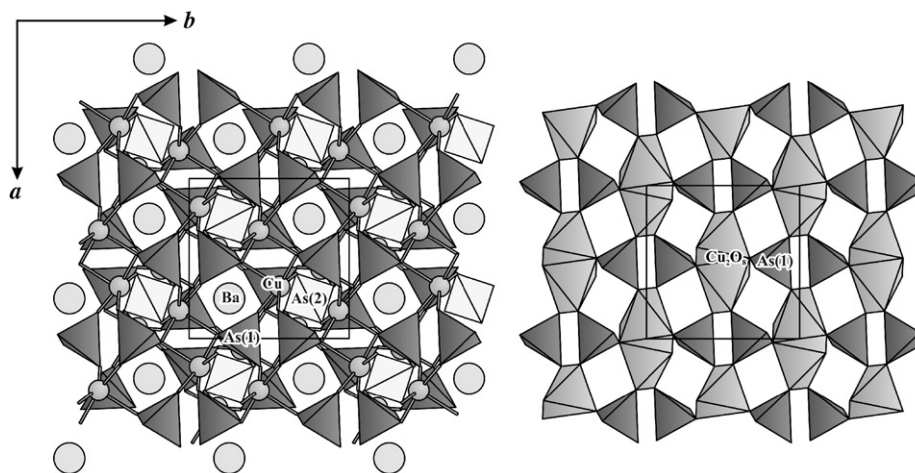

Fig. 7. The (001) projections of the crystal structure of **2** and the slab placed approximately between $0.79 < z < 1.21$ and formed by $[Cu_2O_8]$ dimers, crosslinked by As1O_4 tetrahedra.

and 1.691 Å. The As1 atom lies on a general position and the As2 atom has site symmetry $\bar{4}$. The individual As1–O bond lengths in the As1O$_3$OH polyhedron vary from 1.664(2) to 1.687(2) Å, but the As1–O5 bond is 1.721(2) Å, which is distinctly longer and suggest the presence of OH group. Though the experimental location of

Table 5
Selected bond distances (Å) and bond angles (°) for the coordination polyhedra in **2** for the room temperature data collection

Ba–O4	2.758(2)	Cu–O2^{ii}	1.899(2)	As1–O2	1.664(2)
–O4^i	2.758(2)	–O4^{vi}	1.964(2)	–O1	1.681(2)
–O5	2.824(2)	–O3^{vii}	1.970(2)	–O3	1.687(2)
–O5^i	2.824(2)	–O1^{iv}	2.048(2)	–O5	1.721(2)
–O1^{ii}	2.826(2)	–O3^{viii}	2.309(2)	⟨As1–O⟩	1.688
–O1^{iii}	2.826(2)	⟨Cu–O⟩	2.083	As2–O4^{vi}	1.691(2)
–O3^{iv}	3.100(2)			–O4^{ix}	1.691(2)
–O3^v	3.100(2)			–O4^{ii}	1.691(2)
–O2^i	3.131(2)			–O4	1.691(2)
–O2	3.131(2)			⟨As2–O⟩	1.691
⟨Ba–O⟩	2.928				

Hydrogen bonds

Donor (D)	H atom	Acceptor (A)	D–H	H···A	D–H···A	D···A
O5	H	O5^{iii}	0.88(2)	1.94(6)	139(7)	2.669(4)
		O1^x	0.88(2)	2.45(6)	131(7)	3.102(3)

^{i}-x+3/2, −y+1/2, z; ^{ii}y, −x+1/2, −z+1/2; ^{iii}−y+3/2, x, −z+1/2; ^{iv}−y+1, x−1/2, z−1/2; ^{v}y+1/2, −x+1, z−1/2; ^{vi}−x+1/2, −y+1/2, z; ^{vii}y−1/2, −x+1, z−1/2; ^{viii}−y+1/2, x−1, −z+1/2; ^{ix}−y+1/2, x, −z+1/2; ^{x}−x+3/2, −y+3/2, z.

Fig. 8. Proposed hydrogen-bonding scheme for **2**.

the H atom is not very reliable due to the relatively high atomic numbers of the other atoms within this compound, there is no doubt about the existence of monoprotonated arsenate group and the hydrogen bond O5–H···O5^{vi} (Table 5). In order to keep charge balance, the hydrogen site may not be fully occupied, in this case only 75%, which lead us to the structural formula Ba$_2$Cu$_4$(As2O$_4$)(As1O$_4$)(As1O$_3$OH)$_{3-}$ for **2**. The As1–O5 bond length is somewhat shorter as compared to the average ⟨As–OH⟩ distance of 1.731(2) Å published in [26], indicating partly occupation. The O–As–O angles are consistent with this interpretation. As compared with the ideal tetrahedral angle of 109.47°, O–As(1)–O(5) angles are slightly smaller [98.49(10)–108.05(11))°] and the other O–As(1)–O angles are slightly larger [(110.91(9)–114.16(11)°]. A similar crystal-chemical behavior was found for protonated phosphates [28].

Because of site symmetry of As2, the As2O$_4$ tetrahedron is expectedly much more regular than the protonated one, the O–As2–O angles are 106.61(13) and 110.92(7)°. Sharing all vertices with BaO$_{10}$ and CuO$_5$ coordination polyhedra it contributes to the formation of a framework structure.

Fig. 8 reveals the proposed hydrogen bonding scheme. The OH group (O5) acts as a hydrogen bond donor toward the symmetrically equivalent oxygen O5 and toward oxygen O1. Therefore, this hydrogen bond can be described as bifurcated. The two O···O distances are different: O5···O5^{vi} = 2.669(4) Å is in the range for commonly observed moderately strong hydrogen bonds, whereas the O5···O1^{vii} distance is long, i.e. 3.102(3) Å. Furthermore, O5 acts as a single hydrogen bond acceptor from another symmetrically equivalent O5. The proposed hydrogen-bonding scheme is more or less in accordance with the bond valences. Considering the contribution of non-hydrogen atoms only, it is to be mentioned that bond valences for all oxygen atoms apart from O5 appear somewhat high (Table 6), but can be attributed to the specific bonding environments of these O atoms (Fig. 8). Three of them (O1, O2 and O4) are bonded to As, Ba and Cu, and O3 is bonded to As and two Cu. Although the O5 atom is strongly undersaturated (Table 7), it is the double donor and single acceptor of a hydrogen bonds, resulting in a balanced bond-valence sum for O5.

Although the anisotropies of the displacement parameters and r.m.s. amplitudes (0.0349, 0.014, 0.0065) of the O5 atom are a slightly larger than those of the other four oxygen atoms present in the crystal structure, indicating some disorder, no super-structure reflections violating the extinction rules $h\,k\,0$: $h+k = 2n$

Table 6
Bond valences ν$_{ij}$ (valence units) for **1**

	Sr1	Sr2	Cu1	Cu2	As1	As2	As3	σν$_{ij}$^{a}	H1	H2	H3	H4	H5	σν$_{ij}$^{b}
O11	–	0.32+0.21	–	–	1.37	–	–	1.90	–	–	–	–	–	1.90
O12	0.33	0.29	–	–	1.34	–	–	1.96	–	–	–	–	–	1.96
O13	0.24	–	–	–	1.18	–	–	1.42	–	0.39	–	–	0.18 × 2	1.99
O14	–	0.20	–	–	1.03	–	–	1.23	0.84	–	–	0.11	–	2.18
O21	0.31	0.30	–	–	–	1.28	–	1.90	–	–	–	–	–	1.90
O22	–	0.28	–	0.47	–	1.27	–	2.02	–	–	–	–	–	2.02
O23	0.34	–	–	0.46	–	1.21	–	2.01	–	–	–	–	–	2.01
O24	0.35	–	–	0.48	–	1.21	–	2.04	–	–	–	–	–	2.04
O31	–	0.18	–	0.41	–	–	1.30	1.89	–	–	0.12	–	–	2.01
O32	0.25	–	0.42 × 2↓	–	–	–	1.23	1.90	–	–	–	–	–	1.90
O33	0.11	–	0.51 × 2↓	0.15	–	–	1.21	1.98	–	–	–	–	–	1.98
O34	0.19	–	–	–	–	–	1.19	1.38	–	0.61	–	–	–	1.99
OW1	–	0.25	–	–	–	–	–	0.25	–	–	0.88	0.89	–	2.02
OW2	–	–	–	–	–	–	–	0	0.16 × 2	–	–	–	0.82 × 2	1.96
Σν$_{ij}$	2.12	2.03	1.86	1.97	4.92	4.97	4.93		1.00	1.00	1.00	1.00	1.00	

The calculation is based on the parameters given in [40] for the hydrogen bonds according to [41].
^{a} Neglecting the contribution from the hydrogen bonds.
^{b} Including the contribution from the hydrogen bonds.

and $0\,0\,l$: $l = 2n$ or indications for a larger cell were observed. The structure refinement of the data collected at 120 K did not reveal significant changes and did not indicate any phase transition.

Table 7
Bond valences v_{ij} (valence units) for **2** for the room temperature data collection

	Ba	Cu	As1	As2	Σv_{ij}
O1	0.24 × 2	0.37	1.26	–	2.11
O2	0.10 × 2	0.55	1.32	–	2.07
O3	0.11 × 2	0.45/0.18	1.24	–	2.09
O4	0.28 × 2	0.46	–	1.22	2.16
O5	0.23 × 2	–	–	1.13	1.59
Σv_{ij}	1.92	2.01	4.95	4.91	

The calculation is based on the parameters given in [40], for the hydrogen bonds according to [41].
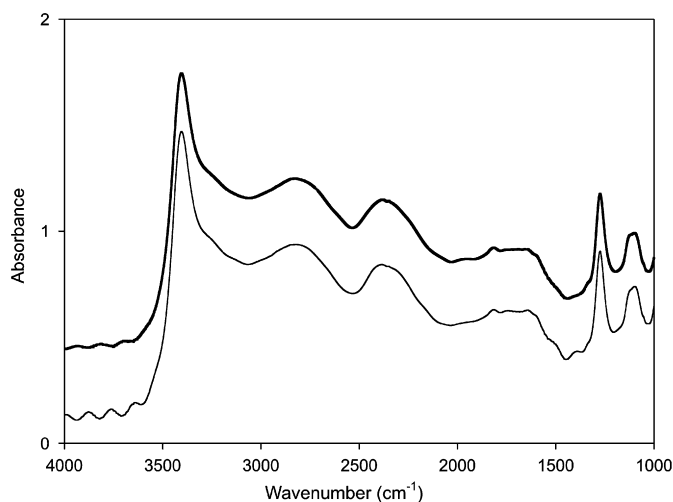

Fig. 9. Single-crystal infrared spectra of **2**. Bands $<1000\,\text{cm}^{-1}$ truncated due to strong absorption.

To obtain further information on the anion groups and especially on hydrogen bonds polarized single-crystal infrared (4000–$530\,\text{cm}^{-1}$) and Raman spectra (4000–$70\,\text{cm}^{-1}$) were acquired (Figs. 9 and 10). Both the IR and the Raman spectra reflect the complexity of the crystal structure. The distinct frequency ranges may be assigned as follows: The three intensity peaks at ca. 2815, 2369 and $1716\,\text{cm}^{-1}$ (Fig. 9) are recognized as the ABC triplet, a well-known phenomenon in spectroscopy of acid oxy-salts. Claydon and Sheppard [37] showed that the so-called ABC structure is formed due to the Fermi resonance between the overtones of δOH and γOH and the stretching vibrations νOH of hydrogen bond [38]. Rather than three unrelated bands, the triplet presents a band profile which is commonly believed to result from Fermi resonance interactions between a broad νOH stretching band and relatively narrow and weak bands of the 2δOH in-plane and 2γOH out-of-plane bending overtones. In **2** the ABC triplt in the infrared spectrum is characteristic of the hydrogen bond O5–H···O1^x ($x = -x$+3/2, $-y$+3/2, z), while the strong peak in infrared and a very weak in the Raman spectrum at $3405\,\text{cm}^{-1}$ is in excellent agreement with the H···O5^{iii} ($iii = -y$+3/2, x, $-z$+1/2) distance of 1.94(6) Å [35]. The δOH banding vibrations are observed at 1276 and $1110\,\text{cm}^{-1}$.

Due to the strong absorption, bands below $\sim 1000\,\text{cm}^{-1}$ are truncated in infrared spectra and therefore could not be discussed (it was not enough material for the powder IR measurement). In the 1000–$700\,\text{cm}^{-1}$ range, Raman spectra show the As–O stretching modes of the $(\text{AsO}_3\text{OH})^{2-}$ and $(\text{AsO}_4)^{3-}$ groups. The intense bands around 898, 870 and $847\,\text{cm}^{-1}$ correspond to the symmetric stretching vibrations of $(\text{AsO}_4)^{3-}$ and $(\text{AsO}_3\text{OH})^{2-}$ groups. The intense band at $810\,\text{cm}^{-1}$ represents the antisymmetric stretching mode of the protonated arsenate group [9].

In the region below $550\,\text{cm}^{-1}$ appear the bending modes of the $(\text{AsO}_3\text{OH})^{2-}$ and $(\text{AsO}_4)^{3-}$ groups, and various low-energetic lattice modes of the compound.

4. Conclusion

Two new copper arsenates, strontium copper(II) hydrogen arsenate(V) trihydrate, $\text{Sr}_4\text{Cu}_3(\text{AsO}_4)_2(\text{AsO}_3\text{OH})_4 \cdot 3\text{H}_2\text{O}$ (**1**) and barium copper(II) hydrogen arsenate (V) $\text{Ba}_2\text{Cu}_4(\text{AsO}_4)_2(\text{AsO}_3\text{OH})$
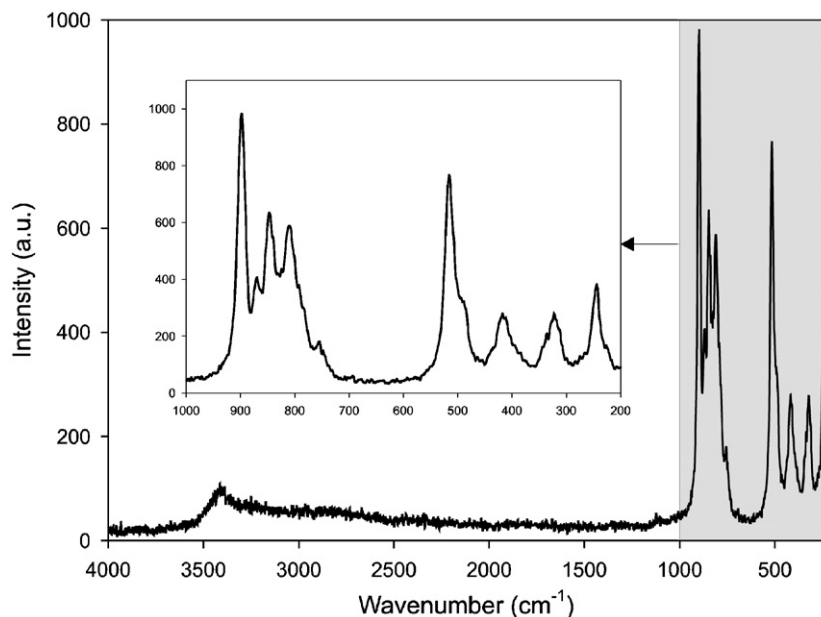

Fig. 10. Raman spectra of **2**.

(**2**) were synthesized using hydrothermal method. Their crystal structure and vibrational spectra were discussed in detail. **1** and **2** represent first compounds in the MO–CuO–As_2O_5–H_2O ($M =$ Sr, Ba) systems, respectively. Furthermore, they both adopt new structure types. This work has demonstrated that synthesis of divalent metal arsenates by low-temperature hydrothermal method can still yield novel structure types with interesting crystal-chemical properties, such as very short hydrogen bond length, where the donor and acceptor are crystallographically different in **1** and ABC-like spectra and existence of the Cu_2O_8 dimer in **2**.

Thorough investigation of the selected metal–arsenate systems would lead to a detailed understanding of which topologies and connectivities are likely to form under which conditions (e.g. temperature, pH, ratios of ionic radii, etc.), a knowledge which could also be applied to the similar phosphates and maybe silicates, which technical use is based on special physical and chemical behavior that is intrinsically dependent on their crystal structure.

Acknowledgments

References

[1] T. Đorđević, Mitt. Österr. Miner. Ges. 153 (2007) 40.
[2] T. Mihajlović, 13th Meeting of the Serbian Crystallographic Society, Novi Sad, June 1–3, 2006, Book of Abstract, 18–19, 2006.
[3] T. Đorđević, Electronic book of abstracts, in: 16th Conference of German Crystallographic Society, March 3–6, 2008, Erlangen, Germany, 1B-05.
[4] T. Đorđević, S. Kovač, Lj. Karanović, Electronic book of abstracts, in: 15th Conference of German Crystallographic Society, March 5–9, 2007, Bremen, Germany, id048, 2007.
[5] T. Đorđević, E. Tillmanns, Abstract Volume, Frontiers in Mineral Sciences, vol. 99, Cambridge, UK, 2007.
[6] T. Đorđević, Lj. Karanović, 14th Meeting of the Serbian Crystallographic Society, Vršac, June 28–30, 2007, Book of Abstract, 34–35, 2007.
[7] T. Mihajlović, H. Effenberger, Z. Kristallogr. 221 (2006) 770–781.
[8] T. Mihajlović, H. Effenberger, Miner. Mag. 68 (2004) 757–767.
[9] T. Mihajlović, E. Libowitzky, H. Effenberger, J. Solid State Chem. 177 (2004) 3963–3970.
[10] T. Mihajlović, U. Kolitsch, H. Effenberger, J. Alloys Compd. 379 (2004) 103–109.
[11] R. Basso, A. Palenzona, L. Zefiro, Neues Jahrb. Mineral. Monatshe. 1989 (1989) 300–308.
[12] R. Basso, L. Zefiro, Neues Jahrb. Mineral. Monatshe 1994 (1994) 205–208.
[13] M.M. Qurashi, W.H. Barnes, Can. Mineral. 7 (1963) 561–577.
[14] J.E. Taggart, E.E. Foord, Miner. Rec. 11 (1980) 37–38.
[15] A.L. Groat, F.C. Hawthrone, Am. Mineral. 75 (1990) 1170–1175.
[16] H. Effenberger, J. Solid State Chem. 142 (1999) 6–13.
[17] Z. Ma, R. He, X. Zhu, Dizhi Xuebao 4 (1990) 302–308.
[18] A.S. Karpov, J. Nuss, M. Jansen, P.E. Kazin, Y.D. Tretyakov, Solid State Sci. 5 (2003) 277–1283.
[19] B.I. Lazoryak, N. Khan, V.A. Morozov, A.A. Belik, S.S. Khasanov, J. Solid State Chem. 145 (1999) 345–355.
[20] T.C. Chen, S.L. Wang, J. Solid State Chem. 121 (1996) 350–355.
[21] Z. Otwinowski, W. Minor, Meth. Enzymol. 276 (1997) 307.
[22] Z. Otwinowski, D. Borek, W. Majewski, W. Minor, Acta Crystallogr. A 59 (2003) 228.
[23] G.M. Sheldrick, SHELXS-97, A Program for the Solution of Crystal Structures, University of Göttingen, Germany, 1997.
[24] G.M. Sheldrick, SHELXL-97, A Program for Crystal Structure Refinement, University of Göttingen, Germany, 1997.
[25] H. Effenberger, J. Solid State Chem. 73 (1988) 118–126.
[26] J. Emsley, Chem. Soc. Rev. 9 (1984) 91.
[27] G. Ferraris, G. Ivaldi, Acta Crystallogr. B 40 (1984) 1–6.
[28] W.H. Baur, Acta Crystallogr. B 30 (1974) 1195–1215.
[29] A.G. Nord, P. Kierkegaard, T. Stefanidis, J. Baran, Chem. Commun. Univ. Stockholm 5 (1988) 1–40.
[30] D. Nyfeler, C. Hoffmann, T. Armbruster, M. Kunz, E. Libowitzky, Am. Mineral. 82 (1997) 841–848.
[31] V.M.F. Hammer, E. Libowitzky, G.R. Rossman, Am. Mineral. 83 (1998) 569–576.
[32] A. Beran, G. Giester, E. Libowitzky, Mineral. Petrol. 61 (1997) 223–235.
[33] A. Novak, Struct. Bond. 18 (1974) 177–216.
[34] V. Szalay, L. Kovács, M. Wöhlecke, E. Libowitzky, Chem. Phys. Lett. 354 (2002) 56–61.
[35] E. Libowitzky, Monatshe. Chem. 130 (1999) 1047–1059.
[36] A. Pujana, J.L. Pizzarro, L. Letama, A. Goni, M.I. Arriortua, T. Rojo, J. Mater. Chem. 8 (1998) 1055–1060.
[37] M.F. Claydon, N. Sheppard, Chem. Commun. 23D (1969) 1431–1433.
[38] S. Bratos, L. Lascombe, A. Novak, OH stretching band of hydrogen-bonded systems in condensed phases, in: H. Ratajczak, W.J. Orville-Thomas (Eds.), Molecular Interactions, Wiley, Chichester, 1980.
[39] R.X. Fischer, E. Tillmanns, Acta Crystallogr. C 44 (1988) 775–776.
[40] N.E. Brese, M. O'Keeffe, Acta Crystallogr. B 47 (1991) 192–197.
[41] G. Ferraris, G. Ivaldi, Acta Crystallogr. B 44 (1988) 341–344.
[42] E. Dowty, ATOMS 6.1, A Computer Program. Kingsport, TN, 1999.